Journal of Photochemistry and Photobiology A: Chemistry 214 (2010) 257–263

Contents lists available at ScienceDirect

Journal of Photochemistry and Photobiology A: Chemistry

journal homepage: www.elsevier.com/locate/jphotochem

Removal of sunscreen compounds from swimming pool water using self-organized TiO_2 nanotubular array electrodes

Jennifer Lynne Esbenshade[a], Juliano Carvalho Cardoso[b], Maria Valnice Boldrin Zanoni[b,*]

[a] Messiah College, Grantham, PA, USA
[b] Departamento de Química Analítica, Instituto de Química, Universidade Estadual Paulista, Av. Prof. Francisco degni, s/n, C. P. 355, 14801-970 Araraquara, SP, Brazil

ARTICLE INFO

Article history:
Received 17 December 2009
Received in revised form 24 June 2010
Accepted 6 July 2010
Available online 13 July 2010

Keywords:
Sunscreens degradation
Photoelectrocatalytic process
TiO_2 nanotubular arrays
4-Methylbenzylidene camphor
3-Benzophenone
3,4-Aminobenzoic acid

ABSTRACT

An alternative method to remove sunscreen compounds 4-methylbenzylidene camphor (4-MBC), 3-benzophenone (BENZO) and 4-aminobenzoic acid (PABA) from swimming pool water is proposed based on photoeletrocatalytic oxidation using self-organized TiO_2 nanotubular array electrodes irradiated by UV light. The best condition for the mineralization of these compounds was found to be 0.1 mol L^{-1} Na_2SO_4 at pH 9 with +1.5 V potential applied to the electrode. This leads to 100% removal of the 4-MBC, BENZO and PABA compounds in tap water, monitored by spectrophotometric and HPLC measurements and a maximum of 98.7%, 90.8% and 88.4% TOC reduction after a 3-h period of treatment. The method was successfully applied to sunscreen degradation in swimming pool water, reaching 100% degradation and 89.5–98.7% TOC reduction, indicating that the method could be an excellent alternative method to produce truly clean water.

1. Introduction

Cosmetic sunscreens have been used for over 75 years as protection from skin photodamage [1]. These sunscreens are comprised of various organic compounds – often called UV filters – that are capable of absorbing UV-B (290–320 nm) and UV-A (320–400 nm) wavelengths, and are added to creams, shampoos, hair sprays, hair dyes, lipsticks, skin lotions, and many more products, to prevent skin damage [2,3]. Although their beneficial effects are known, use of UV filter containing products has been correlated with dermatological problems [4–7] and undesirable estrogenic and antithyroid effects [8–10]. Therefore, many countries have limited its presence in cosmetic products and surface waters by setting maximum safety measures [4–6].

But, warm weather brings increased activity in water as well as an increased application of sunscreen products. Increasingly aware of the potential side effects of these compounds, the concentration of sunscreens that accumulates in swimming pools and other water sources need to be considered. The water resistance of typical sunscreens is very low, retaining only 10–30% of the cream on the skin after one immersion in water [11,12]. Additionally, research conducted at 14 wastewater treatment plants in Switzerland found concentrations in sewage sludge as high as 1780 μg/kg for 4-methylbenzylidene camphor (4-MBC), among other UV filters [12]. With concentrations of UV filters accumulating in water sources and swimming pool waters, an efficient method for the degradation of sunscreen compounds in water would be a desirable application.

Alternative methods based on heterogeneous photocatalysis, which rely on the generation of hydroxyl radicals for environmental remediation, have been employed for the treatment of sunscreen in wastewaters [13,14]. The use of filters containing Fe(III)-Pc/TiO_2 modified photocatalyst have adsorbed 80% of 4-aminobenzoic acid (PABA) [13]. Additionally, some authors indicate that the combined effects of TiO_2, H_2O_2, and light intensity presented 80% degradation of 4-MBC [14].

An attractive strategy to increase the photocatalytic efficiency consists of introducing a reverse bias potential to an anode coated by the photocatalyst which is irradiated with UV light. Examples of such photoelectrocatalytic oxidation have been seen applied to organic dyes [15–17]. To increase this efficiency, several authors have used photoelectrocatalysis on anodically grown self-organized TiO_2 nanotubes [17–19]. These nanotubes may be prepared by anodic oxidation of Ti substrate (essentially in any form, e.g., as sheet, foil, wire, etc.) in fluoride containing electrolytes. While growing, the nanotubes remain attached to the substrate. By tailoring the electrochemical conditions, nanotube layers with thickness in the range of a few hundred nm to a few hundred mm can be synthesized using this electrochemical approach [19,20]. The diameter of the nanotubes can be varied in

* Corresponding author.
E-mail address: boldrinv@iq.unesp.br (M.V.B. Zanoni).

1010-6030/$ – see front matter © 2010 Elsevier B.V. All rights reserved.
doi:10.1016/j.jphotochem.2010.07.005

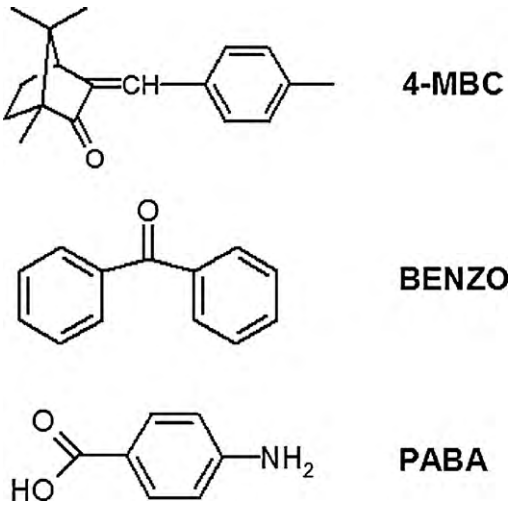

Fig. 1. Chemical structures of 4-methylbenzylidene (4-MBC), benzophenone-3 (BENZO) and 4-aminobenzoic acid (PABA).

the range of 20–300 nm. The large surface area of the nanotubular array (NTA) structure and the vectorial charge transport can enhance the efficiency of light energy conversion and maximize the number of photogenerated electron–hole pairs. Therefore, higher photoelectrocatalytic efficiency has been observed [18]. Although, much research has been conducted on the degradation of various pharmaceutical compounds and dyes in aqueous solutions by photocatalysis [13,21–23], there is little research in the photodegradation of sunscreens for the purpose of mineralizing their components from swimming pool water.

This study explores the application of a titanium dioxide nanotubular array electrode applied to the photoelectrochemical oxidation of several commercial sunscreen compounds, 4-methylbenzylidene camphor (4-MBC), benzophenone (BENZO), and 4-aminobenzoic acid (PABA), for which chemical structures are shown in Fig. 1. The pH, supporting electrolyte, and initial concentration of sunscreen compound were optimized for the most effective results as monitored by UV–vis spectrophotometry, total organic carbon (TOC), and high performance liquid chromatography coupled to a diode array detector (HPLC-DAD). Additionally, the method was successfully applied for swimming pool water spiked with 4-MBC, BENZO, and PABA to examine for the potential application of this process to swimming pool water treatment.

2. Experimental

2.1. Reagents

The chemical filters MBC (Eusolex 6300; purity >99%), BENZO (Eusolex 4360; purity >99%), and PABA (purity 98%) all from Merck (Darmstadt, Germany), were prepared by direct weighing in order to obtain a 1.0×10^{-2} mol L^{-1} stock solution dissolved in methanol for MBC and BENZO and in water for PABA, followed by a dilution to a concentration of 1.0×10^{-4} mol L^{-1}. The supporting electrolyte was prepared by directly weighing Na_2SO_4 (Merck) and dissolution to a concentration of 0.1 mol L^{-1} in purified water. Additional support electrolytes were prepared similarly using NaCl (J.T.Baker) and $NaNO_3$ (Merck). The solutions had their pH adjusted by sodium hydroxide solution (Merck). All reagents were of analytical grade. The deionized water was purified with a Milli-Q plus system (Millipore, Bedford, MA, USA). Methanol (HPLC grade) and acetic acid, both from Merck were used for the chromatographic analysis.

2.2. Photoelectrode

Titanium foil (99.95%, Alfa Aesar), 0.25 mm thick, was polished to a mirror quality smooth finish using silicon carbide sandpaper of successively finer roughness (220, 320, 400, 500, 1200, and 1500 grit) and degreased by successively sonicating for 15 min in isopropanol, acetone and finally ultrapure water. The foil was then dried under a flowing N_2 stream and used immediately. Highly ordered TiO_2 nanotube arrays were prepared by a potentiostatic anodization in a two-electrode electrochemical cell. A titanium foil of size 5 cm × 5 cm was used as a working electrode, and a platinum foil of size 2 cm × 2 cm served as a counter electrode. The distance between the working electrode and the counter electrode was about 2 cm. A voltage was applied by a DC power supply (model MQ of Microquímica, Brazil). The TiO_2 nanotubular array was formed by anodizing the Ti foil in 150 mL of organic electrolyte, which showed a dependence on the anodization time. The organic electrolyte was 0.25% ammonium fluoride (97.0%, Fisher) in glycerol (98.5%, Fisher) containing 10% volume Milli-Q water. The grown porous layers were annealed at 450 °C for 30 min in a furnace (model 650-14 Isotemp Programmable Muffle Furnace, Fisher Scientific) and were allowed to cool gradually back to the ambient condition. The efficiency of the nanotubular electrode was compared with a nanoporous electrode. This electrode was prepared as in reference [24].

2.3. Apparatus

2.3.1. Voltammetry

Electrochemical analyses were performed using an Autolab 302 Potentiostat/Galvanostat (Utrecht, The Netherlands). A three-electrode system consisted of self-organized TiO_2 nanotubular array as the working electrode with a surface area of 25 cm^2, an Ag/AgCl reference electrode and a platinum auxiliary electrode. A potentiostat/galvanostat interfaced with a microcomputer running general purpose electrochemical system (GPES) software (Eco Chemie BV, Utrecht, The Netherlands) was used for acquisition and subsequent analysis of voltammetric data. All pH measurements were made using a combined glass electrode (BlueLine; Schott, Mainz, Germany) connected to a digital pH meter (Alpha model; Schott, Mainz, Germany).

2.3.2. Degradation experiments

The photoelectrocatalytic (PEC) experiments were performed in a 250 mL cylindrical glass reactor, with an ultraviolet (UV) irradiation (a 150 W high pressure mercury lamp from Oriel with a maximum wavelength of 365 nm), vertically inserted in a central quartz glass bulb. The counter electrode was a Pt gauze counter electrode and a saturated Ag/AgCl was used as the reference electrode, immersed in a Luggin capillary. The working electrode was the TiO_2 nanotube array.

2.3.3. UV–vis spectrophotometry, organic carbon, and HPLC analyses

The absorption spectra in the ultraviolet and visible range were recorded for all samples with a Hewlett-Packard spectrophotometer, model HP 8452A in a 10 mm quartz cell. Total organic carbon analyzer (TOC-VCPN, Shimadzu, Japan) was used to monitor the samples for mineralization.

HPLC analyses were performed with a Shimatzu SCL-10AVP system equipped with a diode array detector. A Shimatzu CLC-ODS C18 column, 25 cm long, 4.6 mm internal diameter, 100 å particle size was used in conjunction with a precolumn of the same material, 1 cm long. The mobile phase used was methanol:water (88:12, v/v). The chromatography was carried out with an injection of 20 μL and a mobile-phase flow rate of 1.00 mL min^{-1} at room temperature.

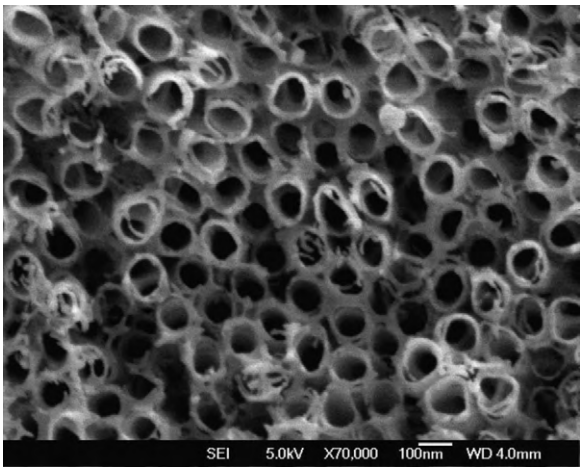

Fig. 2. FEG-SEM images of titania nanotubes prepared by anodization in 10 wt% water + 0.5 wt% NH_4F in glycerol at 30 V for 50 h.

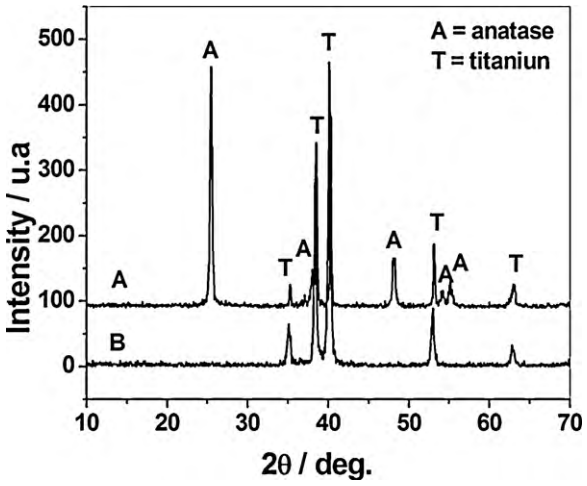

Fig. 3. X-ray diffraction patterns of TiO_2 nanotubular arrays annealed at 450 °C for 30 min (A) and titanium foil (B).

Analysis was performed at the following wavelengths: 287 nm for BENZO, 320 nm for MBC, and 310 nm for PABA.

3. Results and discussion

3.1. Characteristics of the TiO_2 nanotubular array electrode

The first set of experiments was carried out to characterize the growth of nanotubes on Ti foil. The anodizing solution used for the experiments was 0.25% NH_4F, 10% water in glycerol as electrolyte. The experiments were carried out at room temperature (22–25 °C), with an anodization voltage of 30 V. The growth of the TiO_2 nanotubes was monitored by taking FEG-SEM images (Fig. 2). It is clear that TiO_2 layer consists of nanotubular arrays with a uniform tube diameter of about 100 nm and a wall thickness of 10 nm.

The formation of nanotubular arrays was the result of competition reactions involving both the electrochemical oxidation of titanium on the metal surface and the chemical dissolution of the formed TiO_2 layer by fluorides in electrolyte [25–29]. The use of highly viscous neutral electrolytes was adopted to control the steady process [30], promoting the chemical drilling at the bottom of the nanotubes. On the other hand, the use of NH_4F as a neutral electrolyte creates a mild anodic oxidizing environment, which essentially minimizes the rate of chemical dissolution of the TiO_2 nanotube wall in comparison with acidic solutions [25]. As a result it is possible to generate TiO_2 films ordered architecture, which can provide a unidirectional electric channel on the catalyst which improves the photoactivity.

Fig. 3 shows the XRD patterns of the TiO_2 nanotubular arrays and TiO_2 nanoparticles prepared as listed in the reference [30], after being annealed at 450 °C under ambient air for 30 min. For reference, the pattern of pure titanium metal is also listed. The diffraction peaks at about 2θ) 25.5°, 37.3°, 38.1°, 48.2°, 54.2°, and 55.2° can be indexed to the (1 0 1), (1 0 3), (0 0 4), (2 0 0), (1 0 5), and (2 1 1) crystal faces of anatase TiO_2.

It is necessary to note that the rutile peak is much lower than the anatase peak, so it is reasonable to neglect the influence of such trace rutile content on the TiO_2 nanotubular arrays. Taking into account that the anatase form has a higher activity than other forms because it preserves more OH active surface sites. This is a good indicator that the TiO_2 nanotubular arrays could contribute significantly to the photoactivity.

Photoelectrochemical activity was analyzed by immersing the TiO_2 nanotubular array electrode in 0.1 M Na_2SO_4 irradiated by a UV light. The photocurrent density was obtained by recording linear sweep voltammograms at 5 mV s^{-1}. This electrode was compared with a nanoporous electrode to observe the effect of the structure on the efficiency (Fig. 4). Under dark conditions (Fig. 4A) there was no obvious current response. But, high photocurrent density was greatly increased under UV irradiation above a potential of −0.25 V vs. Ag/AgCl and the current values are constant after reaching a potential of +1.5 V. As shown in Fig. 4, the nanotubular electrode (Fig. 4C) is 6 times more intense than nanoporous TiO_2 electrodes (Fig. 4B). The overall efficiency of electron transfer through the Ti/TiO_2 electrode depends highly on the surface microstructure of the TiO_2 films and its supporting material, which influences the electron transition inside the semiconductor and electron transfer on the interface of the Ti/TiO_2 electrode [31]. Apparently, the experimental results in this study demonstrated that the higher anodic potential caused the higher current response and a significant photocurrent response occurred when the applied potential was above 1.5 V vs. Ag/AgCl. It can be clearly seen that the total photoelectrochemical response current results mostly from the photocurrent, while the contribution from the electrochemical reaction current is very small. The significant enhancement in photoelectrochemical current response can find potential applications in this type of highly ordered TiO_2 nanotubular array.

The photoelectrochemical current density reflects the generation, separation and transfer efficiency of photo-excited electrons

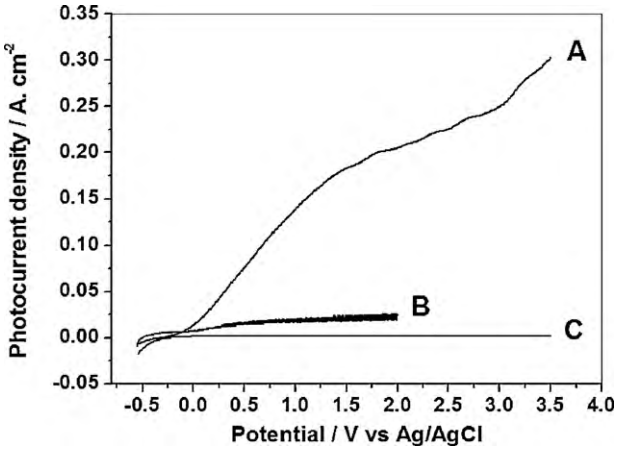

Fig. 4. Photocurrent density vs. applied potential (vs. Ag/AgCl) in 0.1 mol L^{-1} Na_2SO_4 solution. (C) Dark current for each sample; (B) nanoporous TiO_2 array and (A) nanotubular TiO_2 arrays under UV irradiation condition. Scan rate 5 mV s^{-1}.

from the valence to the conduction band of TiO_2. Therefore, the crystallized TiO_2 nanotubular array can act effectively as a novel photoelectrochemical material to be incorporated into promising technological applications, such as a photocatalyst. Since there is superior electron transport, the decreases in the photoelectrocatalytic oxidation efficiency resulting from the recombination process is reduced.

3.2. Application of TiO_2 nanotubular array on photodegradation of 4-MBC sunscreen

The TiO_2 nanotubular array electrode was tested in the degradation of 5×10^{-5} mol L^{-1} of 4-MBC in 0.1 mol L^{-1} Na_2SO_4 at pH 9 by photoelectrocatalytic oxidation operating under UV irradiation and applied potential of 1.5 V. Spectrometric measurements in the UV–vis region displayed two identifying peaks at wavelength 320 and 245 nm (Fig. 5, Curve A). The UV spectrum at various time intervals of the photoelectrocatalytic process was recorded over 180 min of treatment (Fig. 5, Curves B–F). After 30 min of oxidation, a significant decrease in the peak at 320 and 245 nm is observed, concomitantly with the occurrence of a new peak at 260 nm due formation of intermediate compounds. But after 120 min of treatment, no peak remains at 320 or 260 nm, indicating a complete degradation of the 4-MBC (Fig. 5, Curve F).

The monitoring of 4-MBC removal by TOC analysis presents surprising results. After 120 min of treatment, there is 92% reduction in total organic carbon, as shown in Curve A of Fig. 6. These results are much improved and increased to 98% of total organic carbon removal after 180 min. This behavior indicates that the photoelectrocatalytic oxidation on TiO_2 nanotube arrays is promoting both degradation and almost complete mineralization of the organic matter, which is more efficient than existing literature methods for removing this type of organic compound.

These results show that with an applied potential the photoelectrocatalytic decomposition of 4-MBC is greatly improved. When an electrical potential is applied, the competing process of charge recombination is minimized by the resulting movement of the electrons to the counter electrode. Thus, holes created by the oxidation process may be trapped on the surface in order to create hydroxyl radicals, vital components of the process to degrade UV filters. It is reasonable to conclude that the improved activity in the photoelectrocatalytic process results from an effective electron–hole separation by the applied positive bias, which forms an electric field within the TiO_2 nanotubuar arrays and makes the photogenerated electrons and holes diffuse in reverse directions.

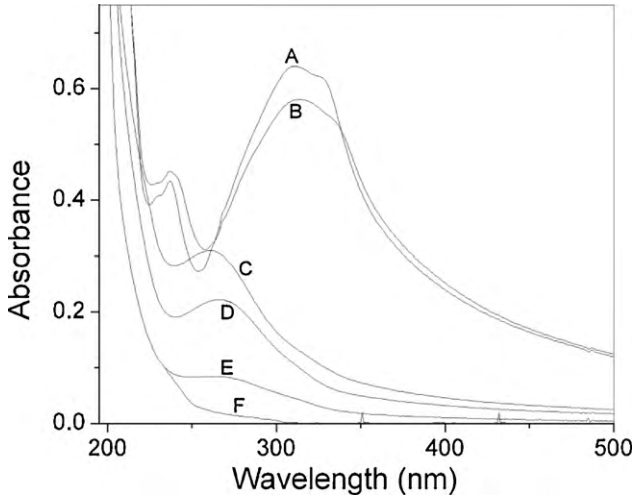

Fig. 5. UV–vis spectra obtained for 5.0×10^{-5} mol L^{-1} 4-MBC in 0.1 mol L^{-1} Na_2SO_4 pH 9 before (A) and after photoelectrocatalytic treatment under UV irradiation and applied potential of +1.5 V: (B) 10 min, (C) 30 min, (D) 60 min, (E) 90 min and (F) 120 min.

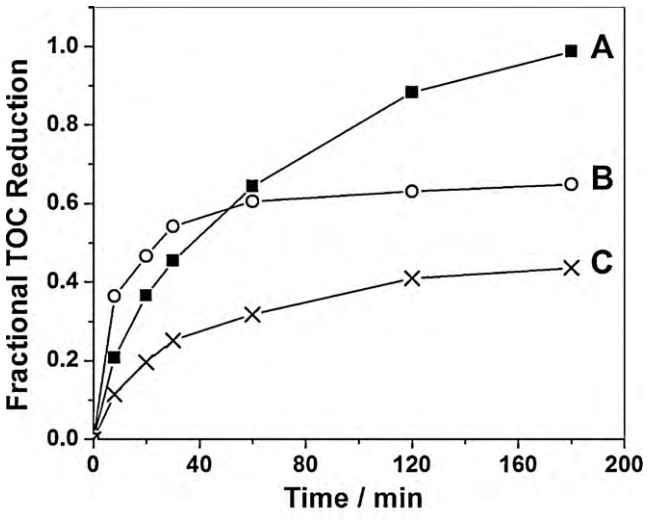

Fig. 6. TOC reduction obtained during photoeletrocatalytic oxidation of 5.0×10^{-6} mol L^{-1} 4-MBC solution under UV irradiation and applied potential of +1.5 V in (A) 0.1 mol L^{-1} Na_2SO_4, (B) 0.1 mol L^{-1} NaCl and (C) 0.1 mol L^{-1} $NaNO_3$.

Further exploration was conducted on the effect of pH, 4-MBC concentration, supporting electrolyte, and different sunscreen compounds with the aim of applying the method to swimming pool water treatment.

3.3. Optimization of the photoelectrocatalytic oxidation method

The supporting electrolyte also plays an important role in a photoelectrochemistry process [32]. The effect of the supporting electrolyte on the performance of TiO_2 nanotubular arrays was tested monitoring the degradation of 5×10^{-5} mol L^{-1} of 4-MBC in 0.1 mol L^{-1} of Na_2SO_4, NaCl and $NaNO_3$. Table 1 shows the maximum values of degradation monitored for the sunscreen signals at 320 nm. Practically all electrolytes promote a total of 93–100% of 4-MBC degradation after 3 h of treatment. Concomitantly, an almost complete vanishing of bands at 240 or 260 nm is observed. However, for TOC reduction, only a Na_2SO_4 solution promotes this reduction efficiently, with 93% of mineralization (Fig. 6, Curve A). In NaCl (Fig. 6, Curve B) and $NaNO_3$ (Fig. 6, Curve C) solutions, there are reductions of only 65% and 44%, respectively, in the TOC measurements. Although, these are significant results and much better than those cited in literature [14], the best supporting electrolyte is sulfate.

These results could be explained by the photolytic reaction of NO_3^- ion to generate nitrite radicals thus decreasing the efficiency of the separation of photogenerated charges [22]. Additionally, sodium chloride can promote a competitive oxidation of chloride ions to chlorine radicals, due h^+ direct oxidation, which also competes with hydroxyl radical formation [22]. Furthermore, the generation of chlorine radicals might generate chlorinated compounds, which would be extremely damaging in the process.

Because the pH of the solution affects both the surface charge of the TiO_2 and the structure of the compound, the result of varying the pH was investigated in the photoelectrocatalytic reduction of 4-MBC. It was found that pH 9 was optimal, achieving complete degradation of the compound and a TOC reduction of 93% for the photoelectrocatalytic process (see Table 1). A pH of 2 was less effective with a photoelectrocatalytic TOC reduction of 82.4%. Therefore, a pH of 9 was chosen as the best experimental condition for further experiments.

Table 1
Influence of concentration of 4-MBC sunscreen, pH and supporting electrolyte solution on the absorbance decay and TOC removal, obtained for the photoelectrocatalytic oxidation of 4-MBC on Ti/TiO_2 nanotubular array electrodes.

	Parameters		Photoelectrocatalytic treatment	
pH	Concentration, 4-MBC (mol L^{-1})	Support electrolyte (0.1 mol L^{-1})	Absorbance decay (320 nm)/%	TOC reduction/%
2	1.00×10^{-5}	Na_2SO_4	98.4	82.4
7	1.00×10^{-5}	Na_2SO_4	100.0	89.1
9	1.00×10^{-5}	Na_2SO_4	100.0	92.8
9	1.00×10^{-5}	Na_2SO_4	100.0	92.8
9	1.00×10^{-5}	NaCl	100.0	64.9
9	1.00×10^{-5}	$NaNO_3$	92.2	43.6
9	5.00×10^{-5}	Na_2SO_4	93.0	46.4
9	1.00×10^{-5}	Na_2SO_4	100.0	92.8
9	5.00×10^{-6}	Na_2SO_4	100.0	98.7

The influence of the starting concentration of the UV filter was considered in order to obtain the best performance from the photoelectrode. The initial concentrations varied between 5×10^{-6} and 5×10^{-5} mol L^{-1} (comparable with levels found in swimming pool water). For this, the supporting electrolyte of 0.1 mol L^{-1} Na_2SO_4 at pH 9 and an applied potential of +1.5 V were kept constant during 120 min of photoelectrocatalytic treatment. Experiments were analyzed for both absorbance decay and TOC reduction (see Table 1).

It was found that the lower concentration of 5×10^{-6} mol L^{-1} 4-MBC was more effectively mineralized, with a complete degradation of absorbance for the process. Likely, there is higher photon absorption on TiO_2 electrode surface coating in diluted solution or adsorption of sunscreen is minimized. Additionally, the TOC reduction reached almost 100% after treatment, indicating complete mineralization. The higher concentration, 5×10^{-5} mol L^{-1} 4-MBC, provided the least degradation with only 46%, only half of that which the lower concentration reduced. When comparing with methods of photocatalysis and electrocatalysis, the results presented TOC reduction of 43.6% and 29.2%, respectively, demonstrating a significant advantage to the developed method. These results suggest that the PEC degradation is a good alternative to treat water containing diluted concentration of sunscreen. This does not compromise the method since the typical concentration of sunscreen in swimming pool water treated periodically does not exceed 1×10^{-4} mol L^{-1}.

3.4. Application of optimized conditions on PABA and BENZO sunscreen compounds

To determine if the photoelectrocatalytic process is as effective on other UV filters as it was for 4-MBC, the optimal conditions for the degradation of 4-MBC were applied to two other commercial sunscreen compounds, PABA and BENZO (chemical structure in Fig. 1). The conditions for all experiments were held at 5×10^{-6} mol L^{-1} of the UV filter in 0.1 mol L^{-1} Na_2SO_4 at pH 9, with applied potential of +1.5 V, using a TiO_2 nanotubular array electrode under UV irradiation. Additionally, a reaction with a mixture of the three UV filters, 4-MBC, PABA, and BENZO, was examined maintaining the original concentration of 5×10^{-6} mol L^{-1} each.

The photoelectrocatalytic treatment of water containing the three sunscreens 4-MBC, PABA and BENZO was also examined by HPLC equipped with a diode array detector. Fig. 7 shows chromatograms recorded for 5.0×10^{-5} mol L^{-1} of each sunscreen of interest and the yielding solutions degraded under photoelectrocatalysis in 0.1 mol L^{-1} sulfate (pH 9) upon UV irradiation. The original solution of sulfate at pH 9 (Curve 0) exhibits three peaks: 4-MBC with a retention time of t_r = 12.6 min (A = 2100); PABA at 10.9 min (A = 250) and BENZO around 6.60 min (A = 6200). HPLC chromatograms of the photoelectrocatalytic degradation of the mixture of UV filters presented degradation of all compounds as well as kinetic information (see Fig. 7). The 4-MBC is the first compound to be completely degraded after only 12 min of photoelectrocatalysis. BENZO is completely degraded after 60 min of the process and the degradation of PABA is maximized at 4 min of photoeletrocatalytic treatment. The photoelectrocatalytic product after 20 min produces a final chromatogram without any peaks corresponding to the UV filter. These results clearly indicate that photoelectrocatalysis promotes a significant mineralization of the sunscreen.

The photoelectrocatalytic process proved to be effective for other UV filters (see Fig. 8). A complete degradation of all compounds was obtained as monitored by maximum absorbance of each compound: 320 nm (4-MBC); 310 nm (PABA) and 287 nm (BENZO). The TOC was also measured and provided values of 88% reduction and 91% reduction for PABA and BENZO, respectively. Additionally, when applied to the combination of the three UV filters, this method produced a 90% of TOC reduction. These results confirm the high efficiency of the TiO_2 nanotubular array on the degradation of sunscreen, independent of its particular chemical composition.

3.5. Analysis of UV filter degradation in swimming pool water

Finally, the method was applied to swimming pool water spiked to 5×10^{-6} mol L^{-1} 4-MBC and also for 5×10^{-6} mol L^{-1} 4-MBC with and without Na_2SO_4 as the supporting electrolyte. Initial

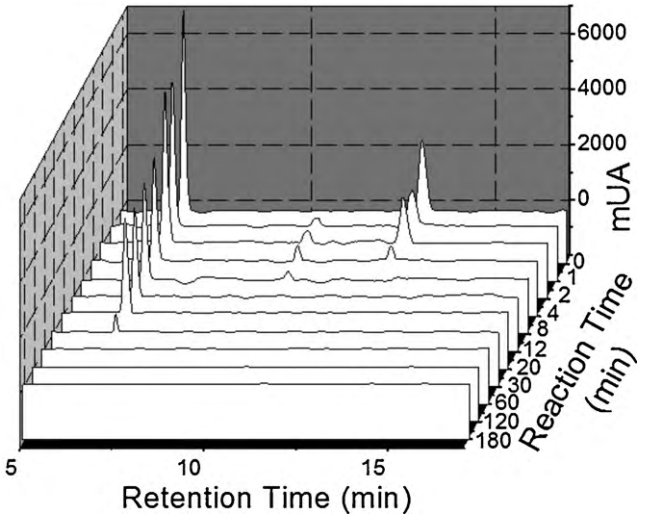

Fig. 7. HPLC chromatograms obtained before (t = 0) and after photoelectrocatalytic oxidation of 4-MBC, BENZO, and PABA solution in 0.1 mol L^{-1} Na_2SO_4 solution pH 9 under UV irradiation and applied potential of +1.5 V. Samples were taken from 0 to 180 min.

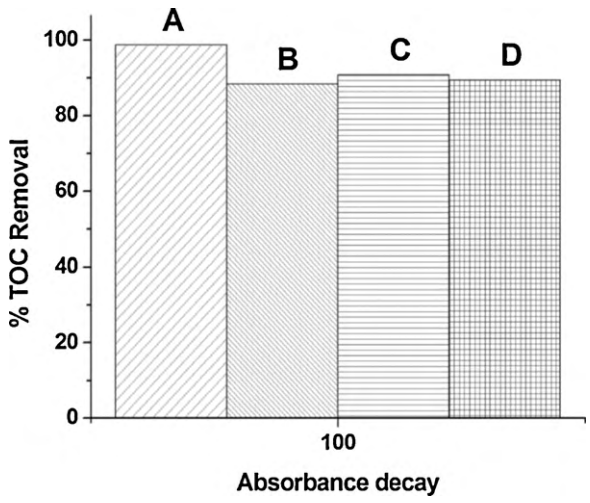

Fig. 8. TOC reduction obtained during photoeletrocatalytic oxidation of 5.0×10^{-5} mol L^{-1} 4-MBC, BENZO and PABA solution under UV irradiation and applied potential of +1.5 V in (A) 4-MBC, (B) PABA, (C) BENZO and (D) mixture of sunscreen.

UV–vis spectroscopy of this water displayed no measurable peaks. The fortified swimming pool water was then treated using the previously determined optimal conditions. The HPLC chromatograms indicate 93% of sunscreen removal after 120 min of treatment for swimming pool water fortified with 4-MBC and 57% TOC removal without the addition of an electrolyte. However, when the swimming pool water was adjusted to 0.1 mol L^{-1} Na_2SO_4 at pH 9, the degradation of 5.0×10^{-6} mol L^{-1} 4-MBC achieved a 100% decay of the compound and a 99% of TOC reduction.

A similar procedure was conducted for swimming pool water fortified with 5.0×10^{-6} mol L^{-1} of 4-MBC, 5.0×10^{-6} mol L^{-1} PABA, and 5.0×10^{-6} mol L^{-1} BENZO with and without pH correction. Maximum mineralization was obtained for BENZO sunscreen in swimming pool water containing Na_2SO_4 with values of 91% TOC reduction, followed by 4-MBC with 90% of TOC removal and 88% for PABA.

4. Conclusion

It has been demonstrated that an efficient mineralization of 4-MBC may be obtained by photoelectrocatalysis conducted on TiO_2 nanotubular array electrodes irradiated by UV light. The pH, supporting electrolyte, and initial concentration of the UV filter all play a role in the effectiveness of the method, with the best conditions obtained with a sodium sulfate electrolyte at pH 9 and a dilute solution of sunscreen. The photoelectrocatalytic process was successfully applied to degrade 4-MBC in swimming pool water without the addition of other chemicals, achieving a 93% degradation of the compound. However, with pH and supporting electrolyte correction a complete mineralization of the compound was obtained along with a 99% TOC reduction. These results show that this photoelectrocatalytic process is more efficient than other alternative treatments based on photocatalytic processes for UV filters. This method has been demonstrated to be applicable in degrading potentially dangerous UV filters from swimming pools. The stability of electrode used presented, after 150 h of photoelectocatalytic treatment, a reduction in the photocurrent intensity of only 20%. Additionally, though the samples analyzed were small scale, the electrodes used in this study have nanotubular array characteristics which cause high surface-to-mass ratios. This attribute allows appropriate scaling for applications in large scale systems more suitable for swimming pool purposes.

Acknowledgments

The authors acknowledge the financial support provided by the Brazilian funding agency FAPESP; LME-LNLS, Campinas, Brazil, for the use of FEG-SEM. Additionally, the Research Experience for Undergraduates (REU) program funded by the NSF/FAPESP made this work possible.

References

[1] F. Urbach, The historical aspects of sunscreens, J. Photochem. Photobiol. B. 64 (2001) 99–104.
[2] D.L. Giokas, A. Salvador, A. Chisvert, UV filters: from sunscreens to human body and the environment, TrAC Trends Anal. Chem. 26 (2007) 360–374.
[3] A. Ziegler, A.S. Jonason, D.J. Leffell, J.A. Simon, H.W. Sharma, J. Kimmelman, L. Remington, T. Jacks, D.E. Brash, Sunburn and p53 in the onset of skin cancer, Nature 372 (1994) 773–776.
[4] European Economic Community Council Directive 76/768, Annex VII, 1976.
[5] US Food and Drug Administration, Fed. Regist. 64 (1999) 27666.
[6] Therapeutic Goods Administration, Aus. Reg. Guidelines for OTC med.2003, 132–145.
[7] T. Schmidt, J. Ring, D. Abeck, Photoallergic contact dermatitis due to combined UVB (4-methylbenzylidene camphor/octyl methoxycinnamate) and UVA (benzophenone-3/butyl methoxydibenzoylmethane) absorber sensitization, Dermatology 196 (1998) 354–357.
[8] M. Schlumpf, B. Cotton, M. Conscience, V. Haller, B. Steinmann, W. Lichtensteiger, In vitro and in vivo estrogenicity of UV screens, Environ. Health Perspect. 109 (2001) 239–244.
[9] C. Schmutzler, I. Hamann, P.J. Hofmann, G. Kovacs, L. Stemmler, B. Mentrup, L. Schomburg, P. Ambrugger, A. Gruters, D. Seidlova-Wuttke, H. Jarry, W. Wuttke, J. Kohrle, Endocrine active compounds affect thyrotropin and thyroid hormone levels in serum as well as endpoints of thyroid hormone action in liver, heart and kidney, Toxicology 205 (2004) 95–102.
[10] S.O Mueller, M. Kling, P.A. Firzani, A. Mecky, E. Duranti, J. Shields-Botella, R. Delansorne, T. Broschard, P. Kramer, Activation of estrogen receptor α and ERβ by 4-methylbenzylidene-camphor in human and rat cells: comparison with phyto- and xenoestrogens, Toxicol. Lett. 142 (2003) 89–101.
[11] D.A. Lambropoulou, D.L. Giokas, V.A. Sakkas, T.A. Albanis, M.I. Karayannis, Gas chromatographic determination of 2-hydroxy-4-methoxybenzophenone and octyldimethyl-*p*-aminobenzoic acid sunscreen agents in swimming pool and bathing waters by solid-phase microextraction, J. Chromotogr. A 967 (2002) 243–253.
[12] C. Plagellat, T. Kupper, R. Furrer, L.F. Alencastro, D. Grandjean, J. Tarradellas, Concentrations and specific loads of UV filters in sewage sludge originating from a monitoring network in Switzerland, Chemosphere 62 (2006) 915–925.
[13] P. Calza, V.A. Sakkas, C. Medana, C. Baiocchi, A. Dimou, E. Pelizzetti, T. Albanis, Photocatalytic degradation study of diclofenac over aqueous TiO_2 suspensions, Appl. Catal. B: Environ. 67 (2006) 197–205.
[14] V.A. Sakkas, P. Calza, M. Azharul Islam, C. Medana, C. Baiocchi, K. Panagiotou, T. Albanis, TiO_2/H_2O_2 mediated photocatalytic transformation of UV filter 4-methylbenzylidene camphor (4-MBC) in aqueous phase: statistical optimization and photoproduct analysis, Appl. Catal. B: Environ. 90 (2009) 526–534.
[15] M.E. Osugi, K. Rajeshwar, D.P. Oliveira, A.R. Araujo, E.R. Ferraz, M.V.B. Zanoni, Comparison of oxidation efficiency of disperse dyes by chemical and photoelectrocatalytic chlorination and removal of mutagenic activity, Electrochim. Acta 54 (2009) 2086–2093.
[16] J.A. Byrne, A. Davidson, P.S.M. Dunlop, B.R. Eggins, Water treatment using nano-crystalline TiO_2 electrodes, J. Photochem. Photobiol. A: Chem. 148 (2002) 365–374.
[17] G. Waldner, J. Krýsa, Photocurrents and degradation rates on particulate TiO_2 layers effect of layer thickness, concentration of oxidizable substance and illumination direction, Electrochim. Acta 50 (2005) 4498–4504.
[18] M.E. Osugi, M.V.B. Zanoni, C.R. Chenthamarakshan, N.R. Tacconi, G.A. Wondemariam, S.S. Mandal, K. Rajeshwar, Toxicity assessment and degradation of disperse azo dyes by photoelectrocatalytic oxidation on Ti/TiO_2 nanotubular array electrodes, J. Adv. Oxid. Technol. 11 (2008) 425–434.
[19] M. Zlamal, J.M. Macak, P. Schmuki, J. Krýsa, Electrochemically assisted photocatalysis on self-organized TiO_2 nanotubes, Electrochem. Commun. 9 (2007) 2822–2826.
[20] V. Zwilling, E. Darque-Ceretti, A. Boutry-Forveille, D. David, M.Y. Perrin, M. Aucoutourier, Structure and physicochemistry of anodic oxide films on titanium and TA6V alloy, Surf. Interface Anal. 27 (1999) 629–637.
[21] V.A. Sakkas, P. Calza, C. Medana, A.E. Villioti, C. Baiocchi, E. Pelizzetti, T. Albanis, Heterogeneous photocatalytic degradation of the pharmaceutical agent salbutamol in aqueous titanium dioxide suspensions, Appl. Catal. B: Environ. 77 (2007) 135–144.
[22] M.V.B. Zanoni, J.J. Sene, M.A. Anderson, Photoelectrocatalytic degradation of Remazol Brilliant Orange 3R on titanium dioxide thin-film electrodes, J. Photochem. Photobiol. A: Chem. 157 (2003) 55–63.
[23] P.A. Carneiro, M.E. Osugi, J.J. Sene, M.A. Anderson, M.V.B. Zanoni, Evaluation of color removal and degradation of a reactive textile azo dye on nanoporous TiO_2 thin-film electrodes, Electrochim. Acta 49 (2004) 3807–3820.

[24] J. Sene, W.A. Zeltner, M.A. Anderson, Fundamental photoelectrocatalytic and electrophoretic mobility studies of TiO_2 and v-doped TiO_2 thin-film electrode materials, J. Phys. Chem. B 107 (2003) 1597–1603.
[25] D. Gong, C.A. Grimes, O.K. Varghese, Titanium oxide nanotube arrays prepared by anodic oxidation, J. Mater. Res. 16 (2001) 3331–3334.
[26] Q. Cai, M. Paulose, O.K. Varghese, C.A. Grimes, The effect of electrolyte composition on the fabrication of self-organized titanium oxide nanotube arrays by anodic oxidation, J. Mater. Res. 20 (2005) 230–236.
[27] K. Shankar, G.K. Mor, A. Fitzgerald, C.A. Grimes, Cation effect on the electrochemical formation of very high aspect ratio TiO_2 nanotube arrays in formamide–water mixtures, J. Phys. Chem. C 111 (2006) 21–26.
[28] M. Paulose, K. Shankar, S. Yoriya, H.E. Prakasam, O.K. Varghese, G.K. Mor, T.A. Latempa, A. Fitzgerald, C.A. Grimes, Anodic growth of highly ordered TiO_2 nanotube arrays to 134 μm in length, J. Phys. Chem. B 110 (2006) 16179–16184.
[29] F. Zhang, S. Chen, Y. Yin, C. Lin, C. Xue, Anodic formation of ordered and bamboo-type TiO_2 anotubes arrays with different electrolytes, J. Alloys Compd. 490 (2010) 247–252.
[30] K. Shankar, G.K. Mor, H.E. Prakasam, S. Yoriya, M. Paulose, O.K. Varghese, C.A. Grimes, Highly-ordered TiO_2 nanotube arrays up to 220 μm in length: use in water photoelectrolysis and dye-sensitized solar cells, Nanotechnology 18 (2007) 065707.
[31] J. Zhao, X. Wang, T. Sun, L. Li, In situ templated synthesis of anatase single-crystal nanotube arrays, Nanotechnology 16 (2005) 2450–2454.
[32] H.O. Finklea, Semiconductor Electrodes, Elsevier, New York, 1988.